Nostradamus: The radar that wanted to be a seismometer

Giovanni Occhipinti,[1,2] Philippe Dorey,[2] Thomas Farges,[3] and Philippe Lognonné[1]

Received 17 May 2010; revised 10 July 2010; accepted 13 July 2010; published 30 September 2010.

[1] Surface waves emitted after large earthquakes are known to induce, by dynamic coupling, atmospheric infrasonic waves propagating upward through the neutral and ionized atmosphere. Those waves have been detected in the past at ionospheric heights using a variety of techniques, such as HF Doppler sounding or GPS receivers. The HF Doppler technique, particularly sensitive to the ionospheric signature of Rayleigh waves is used here to show ionospheric perturbations consistent with the propagation of Rayleigh wave phases R1 and R2 following the Sumatra earthquake on the 28 March 2005 (M = 8.6). This is in our knowledge the first time that the phase R2 is detected by ionospheric sounding. In addition, we prove here that the ionospheric signature of R2 is also observed by over-the-horizon (OTH) Radar. The latter was never used before to detect seismic signature in the ionosphere. Adding the OTH Radar to the list of the "ionospheric seismometers" we discuss and compare the performances of the three different instruments mentioned above, namely HF Doppler sounding, GPS receivers and OTH radar. **Citation:** Occhipinti, G., P. Dorey, T. Farges, and P. Lognonné (2010), Nostradamus: The radar that wanted to be a seismometer, *Geophys. Res. Lett.*, *37*, L18104, doi:10.1029/2010GL044009.

1. Introduction

[2] On March 28, 2005, the over-the-horizon radar prototype Nostradamus wasn't operative. After the first early seismic information (received by cell phone (SGREAMS, Seismic Global Relay, and Event Alert by Mail and SMS, http://ganymede.ipgp.jussieu.fr/~gabsi/)) I (the "I" refer to the first author (G. Occhipinti) who was alone during the measurement of the OTH radar but in contact by cell phone with his co-authors) jumped in a cab to go to the radar control center and catch, at least, the Rayleigh wave phase R2. Surface waves generated by large earthquakes travel around the world several times: we call R1 the first and more energetic wave reaching the observation point A, consequently R2 is the second wave reaching A, after having travelled around the world (Figure 1). We weren't interested in measuring the Rayleigh wave at the surface of the Earth but its signature in the ionosphere. Surface displacement induced by Rayleigh waves is known to produce, by dynamic coupling, an acoustic wave that,propagating upward in the atmosphere, is strongly amplified by the combined effects of the decrease of atmospheric density ρ and the conservation of kinetic energy $E_c = \rho v^2$, where v is the local velocity perturbed by the wave propagation. Reaching the altitude over 80 km the generated acoustic wave interacts with the ionosphere creating strong variations in the plasma velocity and plasma density, detectable by ionospheric sounding (e.g., Doppler sounders, Incoherent Scatter Radar, GPS).

[3] The capability of Doppler sounding to detect the signature of Rayleigh waves in the ionosphere was extensively discussed in the past [*Najita and Yuen*, 1979; *Tanaka et al.*, 1984; *Artru et al.*, 2001, 2004]. Measures of the dispersion of Rayleigh waves performed by Doppler sounding found a clear accord with seismic data [*Najita and Yuen*, 1979], and proved that lithospheric properties are measurable observing the ionosphere at 150 km of altitude. Today, Doppler sounders are able to measure routinely the ionospheric signature of Rayleigh waves for moderate seismic events ($M \geq 6.8$ [*Artru et al.*, 2004]).

[4] Dense GPS networks recently supplied two-dimensional (2D) maps of total electron content (TEC) variations, sufficiently accurate to image the perturbation induced by Rayleigh waves in the ionosphere. These observations allowed to estimate the mean Rayleigh wave propagation velocity [*Ducic et al.*, 2003], as well as source parameters [*Heki et al.*, 2006]. However, as a consequence of the integrated nature of TEC, the GPS sensitivity is limited to extremely large events ($M \geq 7.9$ [*Lognonné et al.*, 2006]). For completeness, we mention that recently similar perturbations are also observed following tsunamis [*Occhipinti*, 2006; *Occhipinti et al.*, 2006, 2008; *Liu et al.*, 2006; *Lee et al.*, 2008].

[5] In this work we principally explore the possibility to detect the Rayleigh wave signature in the ionosphere by over-the-horizon (OTH) radar. This instrument could, in the future, combine the sensitivity of HF Doppler sounder and the imaging-capability of dense GPS networks. Indeed, the OTH radar is able to sound, as dense GPS network, large regions in the ionosphere [*Bazin et al.*, 2006], consequently, it could image in the ionosphere plasma velocity perturbations related to Rayleigh waves, with a very high spatial resolution (~10 km), and with the same sensitivity of the HF Doppler sounder.

2. Doppler Sounding and OTH Radar

[6] Electromagnetic (EM) waves emitted at high frequencies (HF, 3–30 MHz) have the intrinsic property to be reflected/refracted by the ionosphere [e.g., *Schunk and Nagy*, 2000]. The refraction index n of an EM wave propagating into the ionospheric plasma at frequency f_e depends on the electron density N_e following equation (1); where e and m_e are the charge and mass of electrons, ϵ_0 the vacuum permittivity,

[1]Equipe Géophysique Spatiale et Planétaire, UMR 7154, Institut de Physique du Globe de Paris, Université Paris Diderot, CNRS, Saint-Maur-des-Fossés, France.
[2]Office National d'Etudes et de Recherches Aérospatiales, Palaiseau, France.
[3]DAM Ile de France, Commissariatà l'Energie Atomique, Arpajon, France.

0094-8276/10/2010GL044009

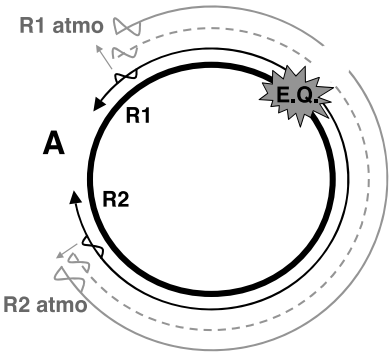

Figure 1. Cartoon of propagation of Rayleigh waves (black) and its signature in the atmosphere (gray) following an Earthquake (E.Q.). R1 is the fist Raylegh wave observed at the point A, R2 is the second Rayleigh wave arriving at the same point after moving around the world following the longer way. The appellation "atmo" shows respectively the signature of R1 and R2 in the atmosphere.

and f_p the plasma frequency. Doppler sounders and OTH radars usually work taking advantage of this reflection/refraction.

$$n = \sqrt{1 - \frac{N_e e^2}{4\pi^2 f_e^2 m_e \epsilon_0}} = \sqrt{1 - \frac{f_p^2}{f_e^2}} \quad (1)$$

The Doppler sounder is generally a bi-static instrument. Short transmitter/receiver distance allows a quasi-vertical sounding, consequently the emitted EM wave is totally reflected in the ionosphere (reflection condition $f_p = f_e$) and the instrument is strictly sensitive to the motion of the reflecting layer [*Davies*, 1990]. The Doppler sounder allows to measure the oscillation velocity of the reflecting layer, by analysis of the Doppler effect on the received signal. The Doppler sounder used in this work is located at Francourville and is managed by CEA [*Blanc and Mercandalli-Rascalou*, 1992; *Farges et al.*, 2003]. The sounding frequency is 3.8 MHz, and the transmitter/receiver distance is 50 km.

[7] OTH radars are primarily designed for detection of hard target (aircrafts and/or ships) for military purpose of air- and oceanic-zone monitoring. EM waves emitted by OTH radar are refracted by ionospheric plasma and go beyond the optical horizon. Consequently, the emitted EM wave follows a curved propagation path traversing ionosphere and propagating until it reaches the ground where it is backscattered. Consequently a part of the emitted signal comes back to the emission point following the same path (Figure 2). There, the residual signal (~14 dB) is detected by the co-located receivers, as the OTH radar Nostradamus (managed by ONERA) used in this work is a mono-static instrument [*Bazin et al.*, 2006].

[8] The variation of group-path of the signal backscattered by the ground is analyzed by FFT sliding-windows to extract the Doppler effect, following the same methodology developed for hard target [*Bazin et al.*, 2006].

[9] For a general overview of the OTH radar Nostradamus see *Bazin et al.* [2006] and Animation S1 of the auxiliary material (courtesy of ONERA (the French Aerospace Lab.), is available at http://www.ipgp.fr/~ninto/NOSTRADAMUS/ONERA_VA.mov).[1]

[10] The OTH radar Nostradamus has a broad EM emission beam (10°–30°), anyway to compare with the Doppler sounder, in this study we consider only the most energetic part of the emission beam. This hypothesis is equivalent to considering a really narrow emission beam. In this study the working frequency f_e is set up at 7.85 MHz.

[11] Supposing the ground unperturbed, the Doppler effect observed on the backscattered signal reveals the oscillation velocity of the ionospheric bouncing layer (reflection condition $f_p = |\sin \alpha| f_e$, where α is the elevation angle of the emitted EM wave). Here, we locate the measurement at the bouncing point, anyway we highlight from now that we know the limit of this hypothesis. Despite the maximum of the sensitivity function (f_e/f_p) - of the emitted EM wave propagating into the ionospheric plasma to the electron density N_e - is located to the bouncing point, the region around that point shows a high sensitivity to the electron density variation (Figure 2).

[12] Additionally, we highlight that the wavelength of the Rayleigh wave is several hundred of kilometers, consequently we suppose that the entire ionosphere moves at the same time. Therefore, the measured Doppler is principally induced by the plasma velocity variation and not by the integration of plasma density variation along the path.

[13] Figure 2 resumes the paths of EM waves emitted by Doppler sounder and OTH radar. The ray path for OTH radar is computed using the ray tracing code TDR [*Occhipinti*, 2006] based on the ionospheric NeQuick model [*Radicella and Leitinger*, 2001].

3. Data Analysis

[14] The ionospheric signature of Rayleigh wave R1 induced by the March 28, 2005, Sumatra earthquake (16:09:36 UT, M = 8.6 (U.S. Geological Survey, Earthquake Hazards Program, 2005, available at http://earthquake.usgs.gov/) reached the European continent at around 17:00 UT, and the phase R2, traveling around the word in the opposite direction, reached the same point ~1.5 hour later (Figure 3).

[15] In Figure 3 (top), the Doppler sounder data (red line) shows clearly the signature of R1 and R2. The signature of R3 (~1.5 hour later then R2) is partially covered by the noise produced by the day/night ionospheric dynamic. The Doppler sounder data are reproduced (black line) by normal mode summation following [*Lognonné et al.*, 1998]. The first arrival phase of R1 is totally described by synthetics (red and black lines are superimposed). Anyway the synthetics do not reproduce the second large signal arriving immediately after R1, partially because of the limit of the 1D model we used to compute synthetics (PREM [*Dziewonski and Anderson*, 1981] for the solid part and USSA [*U.S. Committee on the Extension to the Standard Atmosphere*, 1976] for the atmosphere) and principally because of the ionospheric noise induced by the active ionospheric dynamic during the day-night change.

[16] The blue line in Figure 3 (middle) shows the vertical velocity observed by OTH radar. Also here the data are

[1] Auxiliary materials are available in the HTML. doi:10.1029/2010GL044009.

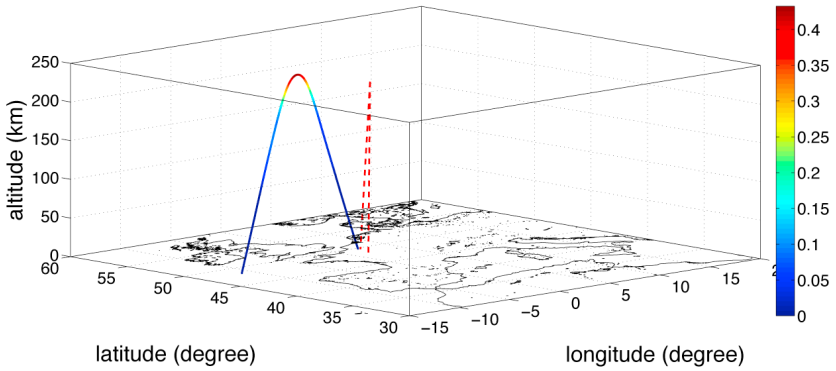

Figure 2. Ray-path of the CEA's Doppler sounder (red dot-line) and the OTH Radar Nostradamus (color line). The Doppler sounder and OTH Radar Nostradamus bouncing points are respectively located at (48.5N, 1.9E, 220.0 km) and (48.7N, −5.2E, 243.4 km). The color in the OTH Radar ray-path indicates a sensitive function f_p/f_e of an EM wave propagating at the frequency f_e in the ionospheric plasma with a plasma frequency f_p.

reproduced by synthetics (black line), particularly well for the phase arriving around 18.6–18.7 UT.

[17] As introduced above, we highlight that OTH radar is treated here as a Doppler sounder, in essence we analyze only the signal coming from the more energetic part of the emission beam. This hypothesis is equivalent to consider a really narrow emission beam.The limit of this hypothesis shows up in the phase arriving around 18.2–18.3 UT that

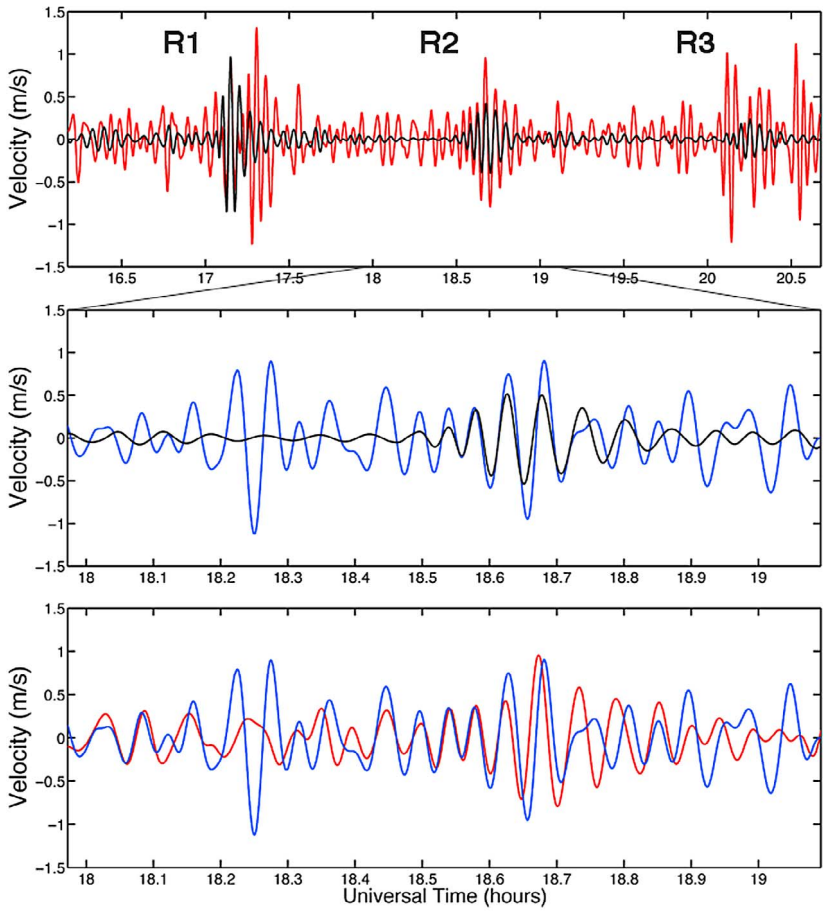

Figure 3. Oscillation of plasma velocity modeled by normal-mode summation (black), and observed by the CEA's Doppler sounding (red) and the OTH Radar Nostradamus (blue). (top) Plasma velocity measured by Doppler sounding (red) and modeled by normal-modes summation (black). Note that in the first arrival of Rayleigh wave R1 around 17.1UT the data and the synthetic are perfectly superimposed. (middle) Plasma velocity measured by OTH radar (blue) and modeled by normal-modes summation (black) within a short time interval centered around R2. (bottom) Doppler sounder and OTH radar data at and around R2. Data and synthetics are filtered between 3–7 mHz.

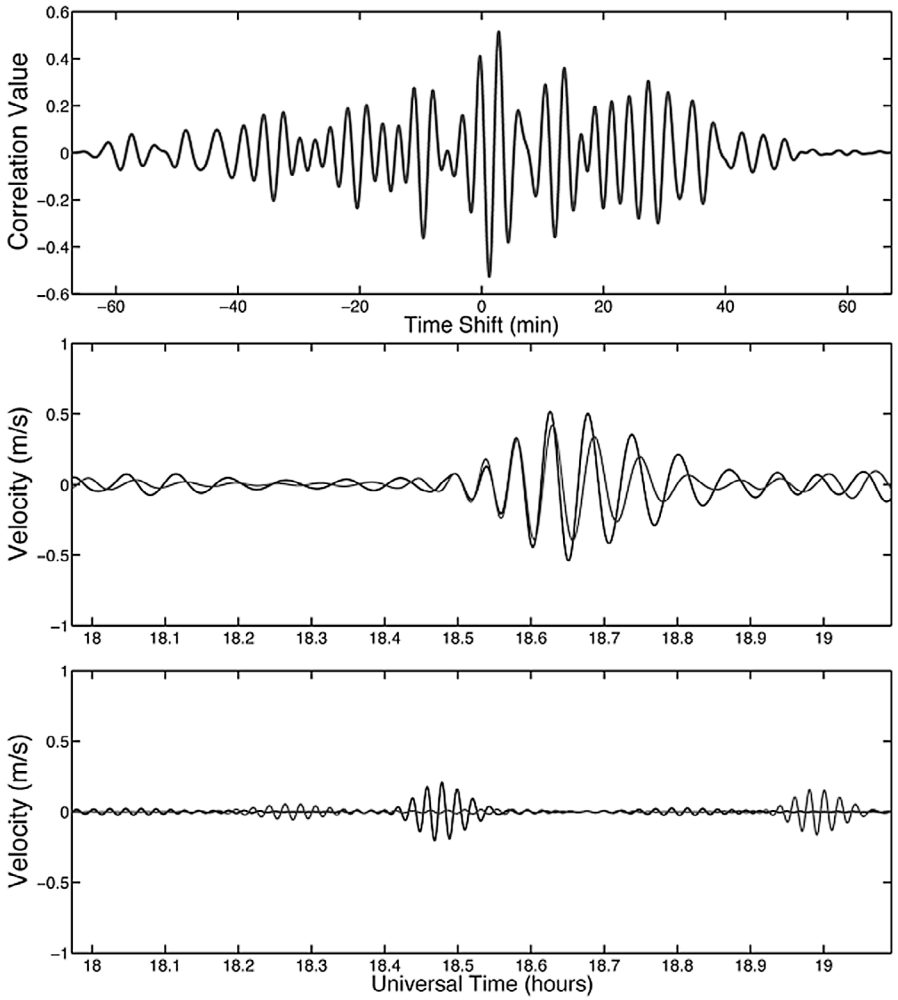

Figure 4. (top) Cross correlation between Doppler sounder and OTH radar data previously filtered between 3–7 mHz. The time-shift links to the maximum correlation value is 2.8 min. (middle) Time-shift of 2.8 min applied to Doppler sounder and OTH radar synthetics. (bottom) Time-shift obtained by cross correlation between Doppler sounder and OTH radar data previously filtered between 10–15 mHz and applied to Doppler sounder and OTH radar synthetics (also filtered in the same range); maximum correlation value obtained filtering data between 10–15 mHz is 0.3.

remains unsolved by the model. This signal could be induced by the less energetic parts of the emission beam or by the finite extension of the sensitivity zone at the ionospheric bouncing point.

[18] Signatures of Rayleigh wave in the Doppler sounder and OTH radar are in agreement (Figure 3, bottom) with a time shift that we can quantify by cross correlation (Figure 4, top). The observed time shift (2.8 min) corresponds to the propagation time that the acoustic wave coupled with the Rayleigh wave needs to propagate from the OTH radar observation point to the Doppler sounder observation point with the horizontal velocity of Rayleigh wave (~3.5 km/s) and the vertical acoustic velocity (~400 m/s). This confirms that both instruments observe the same wave (Figure 4, middle).

[19] Data and synthetics presented here were filtered between 3–7 mHz. If we filter data in a different frequency range (e.g., 10–15 mHz) we obtain a maximum correlation value of 0.3 and an incoherent time shift (Figure 4, bottom). This simple frequency test is in agreement with previous observations suggesting that the transfer of energy between the solid Earth and the atmosphere go through fundamental modes 0S29 and 0S37, at 3.68 mHz and 4.40 mHz respectively [*Kanamori and Mori*, 1992; *Kanamori et al.*, 1994; *Lognonné et al.*, 1998].

4. Conclusions

[20] In this work we show the clear signature of Rayleigh wave phases R1 and R2 observed by ionospheric sounding during the Sumatra event (28 March, 2005).

[21] The detection of both phases R1 and R2 by Doppler sounding confirms the sensitivity of the ionosphere to solid Earth phenomena. Since the '70s, Doppler sounder continues to prove that seismic Rayleigh waves are detectable at teleseismic distances observing the ionosphere at 150–200 km of altitude. Despite its sensitivity to moderate Earthquakes ($M \geq 6.8$), Doppler sounders still sound only one point in the ionosphere and could be compared to a low resolution vertical component seismometer located in the atmosphere.

[22] Today, dense GPS networks allow to image propagation of Rayleigh wave in the ionosphere with a high spatial

resolution. Unfortunately, as a consequence of the integrated nature of TEC, the sensitivity of GPS to the ionospheric solid Earth phenomena is limited to large events ($M \geq 7.9$).

[23] We demonstrated here the capability of OTH radar to measure the signature of Rayleigh waves in the ionosphere with the same sensitivity of Doppler sounder. We optimistically extrapolate from this result that sensitivity of OTH radar is better than GPS and we hope that future works will confirm it. Detection of Rayleigh wave by OTH radar could open new perspectives in (ionospheric) seismology combining the sensitivity of Doppler sounding and the imaging capability of dense GPS networks. Consequently, OTH radar could measure the arrival time of Rayleigh wave over large regions (200×200 km^2) with high spatial resolution (10 km). In addition, existing OTH radars (Nostradamus, Gindalee, US-OTH radars) cover large oceanic zones where we have, in the best case, only few available seismometers.

[24] This paper wishes to encourage studies on OTH radar and ionospheric seismology to open, in a near future, the seismic data-set to ionospheric sounding.

[25] **Acknowledgments.** This project is supported by ONERA and by CNES. We thank two anonymous reviewers for their constructive remarks; G.O. also thank J.-P. Molinie and J. Munoz for useful discussions. This is IPGP contribution 3044.

References

Artru, J., P. Lognonné, and E. Blanc (2001), Normal modes modelling of post-seismic ionospheric oscillations, *Geophys. Res. Lett.*, *28*, 697–700.

Artru, J., T. Farges, and P. Lognonné (2004), Acoustic waves generetad from seismic surface waves: Propagation properties determined from Doppler sounding observation and normal-modes modeling, *Geophys. J. Int.*, *158*, 1067–1077.

Bazin, V., J. P. Molinie, J. Munoz, P. Dorey, S. Saillant, G. Auffray, V. Rannou, and M. Lesturgie (2006), Nostradamus: An OTH Radar, *IEEE Aerosp. Electron. Syst. Mag.*, *21*(10), 3–11.

Blanc, E., and B. Mercandalli-Rascalou (1992), Mid-latitude ionospheric disturbances produced by major magnetic storms, *Can. J. Phys.*, *70*, 553–565.

Davies, K. (1990), *Ionospheric Radio*, Peter Peregrinus, London.

Ducic, V., J. Artru, and P. Lognonné (2003), Ionospheric remote sensing of the Denali earthquake Rayleigh surface waves, *Geophys. Res. Lett.*, *30*(18), 1951, doi:10.1029/2003GL017812.

Dziewonski, A., and D. L. Anderson (1981), Preliminary reference Earth model, *Phys. Earth Planet. Inter.*, *25*, 297–356.

Farges, T., A. Le Pichon, E. Blanc, S. Perez, and B. Alcoverro (2003), Response of the lower atmosphere and the ionosphere to the eclipse of August 11, 1999, *J. Atmos. Terr. Phys.*, *65*, 717–726.

Heki, K., Y. Otsuka, N. Choosakul, N. Hemmakorn, T. Komolmis, and T. Maruyama (2006), Detection of ruptures of Andaman fault segments in the 2004 great Sumatra earthquake with coseismic ionospheric disturbances, *J. Geophys. Res.*, *111*, B09313, doi:10.1029/2005JB004202.

Kanamori, H., and J. Mori (1992), Harmonic excitation of mantle Rayleigh waves by the 1991 eruption of Mount Pinatubo, Philippines, *Geophys. Res. Lett.*, *19*, 721–724.

Kanamori, H., J. Mori, and D. G. Harkrider (1994), Excitation of atmospheric oscillations by volcanic eruptions, *J. Geophys. Res.*, *99*, 21,947–21,961.

Lee, M. C., R. Pradipta, W. J. Burke, A. Labno, L. M. Burton, J. A. Cohen, S. E. Dorfman, A. J. Coster, M. P. Sulzer, and S. P. Kuo (2008), Did tsunami-launched gravity waves trigger ionospheric turbulence over Arecibo?, *J. Geophys. Res.*, *113*, A01302, doi:10.1029/2007JA012615.

Liu, J.-Y., Y.-B. Tsai, K.-F. Ma, Y.-I. Chen, H.-F. Tsai, C.-H. Lin, M. Kamogawa, and C.-P. Lee (2006), Ionospheric GPS total electron content (TEC) disturbances triggered by the 26 December 2004 Indian Ocean tsunami, *J. Geophys. Res.*, *111*, A05303, doi:10.1029/2005JA011200.

Lognonné, P., E. Clévédé, and H. Kanamori (1998), Computation of seismograms and atmospheric oscillations by normal-mode summation for a spherical Earth model with realistic atmosphere, *Geophys. J. Int.*, *135*, 388–406.

Lognonné, P., J. Artru, R. Garcia, F. Crespon, V. Ducic, E. Jeansou, G. Occhipinti, J. Helbert, G. Moreaux, and P. E. Godet (2006), Ground based GPS imaging of ionospheric post-seismic signal, *Planet Space Sci.*, *54*, 528–540.

Najita, K., and P. C. Yuen (1979), Long-period oceanic Rayleigh wave group velocity dispersion curve from HF Doppler sounding of the ionosphere, *J. Geophys. Res.*, *84*, 1253–1260.

Occhipinti, G. (2006), Observations multi-paramètres et modélisation de la signature ionosphérique du grand séisme de Sumatra, Ph.D. thesis, Inst. de Phys. du Globe de Paris, Paris. (Available at http://www.ipgp.fr/~ninto)

Occhipinti, G., P. Lognonné, E. A. Kherani, and H. Hébert (2006), Three-dimensional waveform modeling of ionospheric signature induced by the 2004 Sumatra tsunami, *Geophys. Res. Lett.*, *33*, L20104, doi:10.1029/2006GL026865.

Occhipinti, G., A. Kherani, and P. Lognonné (2008), Geomagnetic dependence of ionospheric disturbances induced by tsunamigenic internal gravity waves, *Geophys. J. Int.*, *173*, 753–765, doi:10.1111/j.1365-246X.2008.03760.x.

Radicella, S. M., and R. Leitinger (2001), The evolution of the DGR approach to model electron density profiles, *Adv. Space Res.*, *27*, 35–40.

Schunk, R. W., and A. F. Nagy (2000), *Ionospheres*, *Cambridge Atmos. Space Sci. Ser.*, Cambridge Univ. Press, Cambridge, U. K.

Tanaka, T., T. Ichinose, T. Okuzawa, and T. Shibata (1984), HF-Doppler observations of acoustic waves excited by the Urakawa-Oki earthquake on 21 March 1982, *J. Atmos. Terr. Phys.*, *46*, 233–245.

U.S. Committee on the Extension to the Standard Atmosphere (1976), U.S. Standard Atmosphere, 1976, *NASA Tech. Memo. NASA-TM-X-74335*, U.S. Gov. Print. Off., Washington, D. C.

P. Dorey, Office National d'Etudes et de Recherches Aérospatiales, Chemin de la Hunière, F-91761 Palaiseau CEDEX, France.

T. Farges, DAM Ile de France, Commissariat à l'Energie Atomique, Bruyères-le-Châtel, F-91297 Arpajon CEDEX, France.

P. Lognonné and G. Occhipinti, Institut de Physique du Globe de Paris, 4, av. de Neptune, F-94107 Saint-Maur-des-Fossés CEDEX, France. (ninto@ipgp.jussieu.fr)